DOI: 10.5281/zenodo.17052649

CHAPTER 1

Growth and Characterization of mixed Amino-Nitrate Crystal with NLO Application

Shailesh S. Dongare

Department of Physics, S. G. Arts, Science and G. P. Commerce College, Shivle 421401 Maharashtra, India

Corresponding author Email: shaileshd1979@gmail.com

Received: 12 August 2025; Accepted: 02 September 2025; Available online: 04 September 2025

Abstract: Glycine–potassium–calcium nitrate (GPCN), a novel semi-organic nonlinear optical (NLO) crystal, was effectively created and developed utilizing the solution growth technique from an aqueous solution at pH 4.8 under carefully regulated temperature conditions. Within three weeks, transparent single crystals measuring around 8 × 6 × 4 mm³ were produced. The solubility of GPCN in water was thoroughly assessed in order to improve the crystal formation process. The crystal's orthorhombic system affiliation was verified by powder X-ray diffraction examination. Its unit cell volume was 1961.30 Å³, and its lattice parameters were a = 14.827 Å, b = 13.287 Å, and c = 9.954 Å. Amino and nitrate functional groups were detected using Fourier Transform Infrared spectroscopy. Its applicability for opto-photonics applications was demonstrated by UV-Vis spectroscopy, which showed high optical transparency with a cut-off wavelength at 216 nm. Using a Nd:YAG laser operating at 1064 nm and the Kurtz and Perry

Materials Science: Advances in Synthesis, Characterization and Applications (Vol. 1) - Digambar M. Sapkal, Harshal M. Bachhav, Gaurav Mahadev Lohar, Sanjay P. Khairnar (Eds.)

ISBN: 978-93-95369-55-8 (paperback) 978-93-95369-46-6 (electronic) | © 2025 Advent Publishing.

https://doi.org/10.5281/zenodo.17052649

powder technique, the nonlinear optical response was investigated. The results showed a second harmonic generation efficiency of 0.66 times that of potassium dihydrogen phosphate. Current-voltage (I-V) measurements and photoconductivity were further characterizations. The surface morphology of the formed crystals was examined using scanning electron microscopy, and dielectric tests showed that the dielectric constant behaved in a frequency-dependent manner. According to Vickers microhardness testing, the mechanical strength was modest. According to these results, GPCN is a viable option for upcoming photonic and NLO device uses.

Keywords: Crystal growth, GPCN, Structure, Nonlinear optical, Hardness, SHG, VHN, UV transparency.

1. Introduction

The advancement of nonlinear optics (NLO) relies heavily on the identification and development of materials capable of strong interactions with high-intensity light beams. Over the past few years, semi-organic materials have drawn considerable attention for SHG applications, as they unite the mechanical stability of inorganics with the tunable molecular properties of organics. Among them, amino acid-based complexes, particularly those formed with different ionic salts, have demonstrated considerable potential as efficient NLO materials[1,2]. Among them, α-glycine a simple and well-studied amino acid has been widely employed in the synthesis of semi-organic compounds exhibiting dielectric, ferroelectric, nonlinear optical, and photosensitive properties[3,4].

Although purely organic crystals exhibit outstanding optical characteristics, their loosely packed molecular frameworks often limit their thermal and mechanical stability. A proven strategy to overcome this limitation is the incorporation of inorganic components into organic matrices, which significantly enhances mechanical robustness and broadens their applicability in device-oriented technologies. These organic–inorganic hybrid systems combine the high nonlinear optical (NLO) coefficients of organic molecules with the structural stability of inorganic constituents, making them highly attractive for advanced photonic applications such as optical data processing, frequency conversion, image transmission, and optical switching. Among the organic materials used for such hybrids, amino acids—including glycine, L-arginine, and L-histidine—are among the most extensively studied due to their favorable structural and optical properties[5,6].

Glycine crystallizes in three polymorphic forms—α, β, and γ—with α-glycine being the most common and structurally fundamental. In its complexes, such as glycine–sodium nitrate, glycine–silver nitrate, and glycine–calcium nitrate, the zwitterionic nature of glycine is preserved, giving rise to intriguing NLO-active crystal structures. In glycine–sodium nitrate crystals, sodium ions exhibit eight-fold coordination, forming a distorted hexagonal bipyramidal polyhedral geometry. The glycine molecules are interconnected through head-to-tail hydrogen bonds, producing a layered structural arrangement[10].

ISBN: 978-93-95369-55-8 (paperback) 978-93-95369-46-6 (electronic)

Given the strong potential of amino acid–inorganic salt systems for second harmonic generation (SHG) applications, the present study focuses on the synthesis and comprehensive characterization of a new mixed amino-nitrate semi-organic crystal—glycine–potassium–calcium nitrate (GPCN). The crystals were grown from an aqueous solution using the slow evaporation method and subsequently analyzed using a range of techniques, including CHN elemental analysis, energy-dispersive X-ray analysis (EDAX), powder X-ray diffraction (XRD), Fourier-transform infrared (FTIR) spectroscopy, ultraviolet–visible (UV–Vis) spectroscopy, SHG efficiency measurements, I–V characterization, SEM, dielectric studies and Vickers microhardness testing

2. Growth and Solubility

Glycine–potassium–calcium nitrate (GPCN) single crystals were produced from an aqueous solution using the slow evaporation approach. AR-grade α-glycine, potassium nitrate (KNO_3), and calcium nitrate [$Ca(NO_3)_2$] were combined in double-distilled water with molar ratios of 3:0.5:0.5 to create the growth solution. The pH of the saturated solution was measured at 4.8 after 0.5% concentrated hydrochloric acid (HCl) was added to correct the acidity. After three to four weeks of crystallization at room temperature, clear crystals with average sizes of around 8 × 6 × 4 mm^3 were produced (Figure 1). Using the flotation process, the density was found to be 1.632 g/cm^3. According to thermal analysis, it decomposed at around 232 °C and had a melting point of 221 °C. It was found that the solute concentration, which is impacted by the solubility of the substance, determines the crystal size. A constant-temperature bath was used to analyze the solubility of GPCN in distilled water throughout a temperature range of up to 350 K in order to investigate this connection (Figure 2). The findings confirmed ideal circumstances for temperature-assisted crystal formation by demonstrating that solubility rose with temperature. The chemical reaction representing the formation of GPCN may be written as:

$$[NH_2CH_2COOH]_3 + [KNO_3]_{1/2} + [\ Ca(NO_3)_2]_{1/2} + 0.5\%\ HCl \longrightarrow [Ca(NO_3)_2]_{1/2}.[NH_2CH_2COOH]_3.\ [KNO_3]_{1/2}.HCl$$

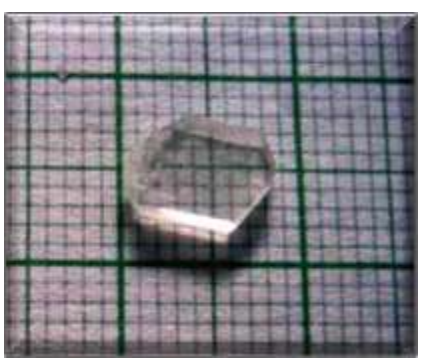

Fig. 1. Grown GPCN Crystal

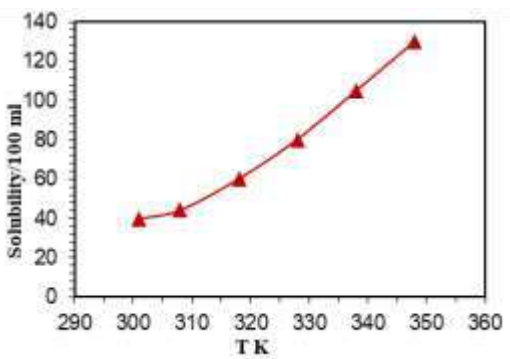

Fig. 2. Solubility curve of GPCN

Materials Science: Advances in Synthesis, Characterization and Applications (Vol. 1) - Digambar M. Sapkal, Harshal M. Bachhav, Gaurav Mahadev Lohar, Sanjay P. Khairnar (Eds.)
ISBN: 978-93-95369-55-8 (paperback) 978-93-95369-46-6 (electronic) | © 2025 Advent Publishing.

3. Characterizations

3.1. CHN and EDAX Analysis

The chemical composition of the synthesized material was determined using CHN elemental analysis and energy-dispersive X-ray analysis (EDAX) performed with a scanning electron microscope[18]. The CHN analysis confirmed the presence of carbon, hydrogen, nitrogen, and oxygen in the sample. The oxygen content was calculated by subtracting the measured percentages of the other elements from the total composition, assuming a sum of 100%. The experimentally obtained results showed excellent agreement with the theoretically predicted values (Table 1). EDAX analysis additionally verified the presence of the key inorganic elements—potassium (K), calcium (Ca), and chlorine (Cl) (Figure 3)—consistent with the proposed molecular formula. The combined CHN and EDAX findings confirm the successful synthesis of the intended GPCN compound.

Table 1. Elemental analysis of GPCN crystal

GPCN	%N	%C	%H	%O	%EDAX Element	Molecular formula
Elements (%)	17.858	30.530	6.328	45.285	K, Ca, Cl	$(KNO_3)_{1/2}\cdot(NH_2CH_2COOH)_3\cdot(Ca(NO_3)_2)_{1/2}$ HCl

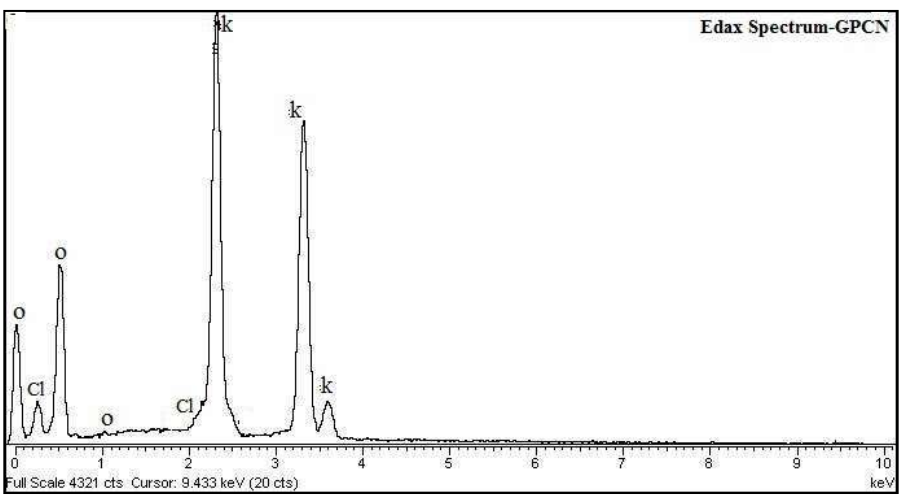

Fig. 3. EDAX Spectra of GPCN crystal.

3.2. XRD Analysis

The structural characteristics and phase purity of the grown GPCN crystal were examined using powder X-ray diffraction (XRD). Measurements were performed on a JEOL diffractometer (JDX-8030 Series) with Cu-Kα radiation (λ = 1.541 Å), scanning over a 2θ range of 10°–80° at a rate of 5° per minute[11,12]. The obtained diffraction patterns were processed and indexed using POWD software (Version 2.2,

ISBN: 978-93-95369-55-8 (paperback) 978-93-95369-46-6 (electronic)

Australia), gives lattice parameters as, a = 14.827 Å, b = 13.287 Å, c = 9.954 Å and the crystal belongs to the orthorhombic symmetry with unit cell volume of 1961.30 Å³. Sharp diffraction peaks were observed, with the most intense peak (12,208 counts) located at 2θ = 29.91°, corresponding to the (4 0 2) plane (Figure 4). A comparison between observed (d_obs) and calculated (d_cal) interplanar spacings showed excellent agreement (Table 2), confirming the high crystallinity and purity of the GPCN sample.

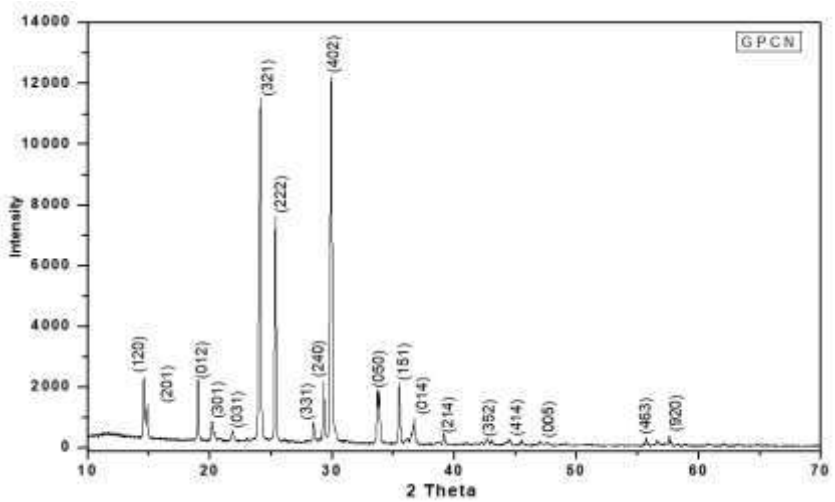

Fig. 4. XRD Spectrum of GPCN sample

Table 2. XRD Assignment of GPCN sample

2theta	Theta	d_{obs} (a.u)	d_{cal}(a.u)	$\Delta d = d_{obs} \sim d_{cal}$ (a.u)	h k l Planes	Intensity
14.60	7.30	6.063	6.063	0.000	1 2 0	2337
14.88	7.44	5.946	5.946	0.000	2 0 1	1454
19.01	9.51	4.661	4.661	0.000	0 1 2	2236
20.13	10.07	4.404	4.426	0.022	3 0 1	893
21.84	10.92	4.065	4.047	0.018	0 3 1	568
24.11	12.06	3.686	3.684	0.002	3 2 1	11501
25.34	12.67	3.511	3.509	0.002	2 2 2	7655
28.45	14.23	3.133	3.131	0.002	3 3 1	866
29.29	14.65	3.045	3.032	0.014	2 4 0	7179
29.91	14.96	2.983	2.973	0.010	4 0 2	12208
33.68	16.84	2.658	2.658	0.000	0 5 0	1975
35.46	17.73	2.529	2.529	0.000	1 5 1	2136
36.71	18.36	2.444	2.446	0.002	0 1 4	974
39.13	19.57	2.323	2.323	0.000	2 1 4	445
42.66	21.33	2.117	2.118	0.001	3 5 2	292

ISBN: 978-93-95369-55-8 (paperback) 978-93-95369-46-6 (electronic) | © 2025 Advent Publishing.

44.43	22.22	2.036	2.041	0.005	4 1 4	322
45.52	22.76	1.990	1.991	0.001	0 0 5	266
55.64	27.82	1.650	1.650	0.000	4 6 3	358
57.57	28.79	1.599	1.599	0.000	9 2 0	388

3.3. ^{1}H and ^{13}C NMR Studies

Nuclear Magnetic Resonance spectroscopy examines the presence of proton and carbon groups in the grown GPCN material. The ^{1}H NMR spectrum was obtained using a Mercury Plus Varian spectrometer operating at 300 MHz, whereas the ^{13}C NMR spectrum was recorded on a Bruker AV-500 spectrometer. These analyses provided detailed information about the chemical environment of hydrogen and carbon atoms within the sample. In the ^{1}H NMR spectrum, characteristic chemical shifts were observed at δ = 4.679 ppm for the amine ($–NH_2$) protons and δ = 3.470/3.468 ppm for the methylene ($–CH_2$) group. The ^{13}C NMR spectrum showed a peak at δ = 172.429 ppm corresponding to the carboxylate ($–COO^-$) group, and another at δ = 41.397 ppm for the $–CH_2$ carbon. These results, confirm the structural integrity of glycine moieties in the GPCN crystal and support the proposed molecular configuration[18].

3.4. FTIR and Raman Studies

The vibrational properties of the grown GPCN crystal were investigated using Fourier Transform Infrared (FTIR) and Laser Raman spectroscopy to identify the functional groups and molecular interactions present in the compound[13],[14]. The FTIR spectrum was recorded in KBr pellet form using a Perkin Elmer 1600 series infrared spectrometer with a resolution of 4 cm^{-1} and a scanning speed of 2 mm/s, covering the range 400–4000 cm^{-1}. Complementary Raman spectra were obtained in the solid state using Raman spectrometer, which cover the 100–3500 cm^{-1} region. As illustrated in Figure 5, the FTIR spectrum displays several characteristic absorption peaks between 400 and 3200 cm^{-1}. Strong IR-active bands dominate the 400–1800 cm^{-1} region, while a broad absorption feature between 1600 and 3100 cm^{-1} indicates the presence of overlapping vibrational modes.

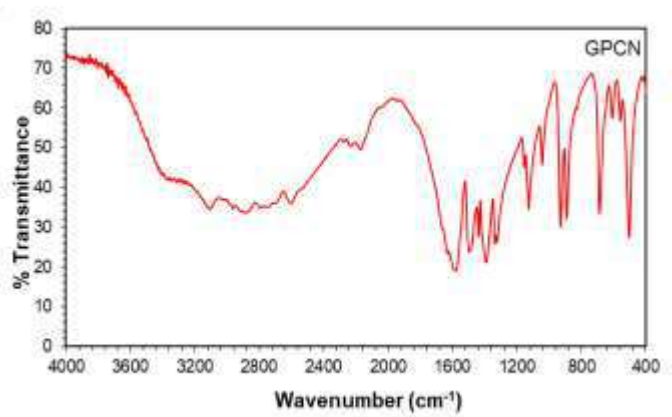

Fig. 5. FTIR Spectrum of GPCN crystal.

ISBN: 978-93-95369-55-8 (paperback) 978-93-95369-46-6 (electronic)

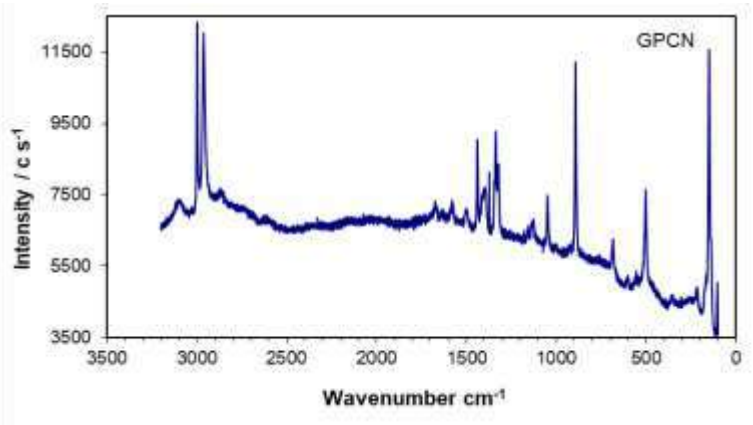

Fig. 6. Raman Spectrum of GPCN crystal.

The presence of glycine in its zwitterion form was confirmed by absorption bands due to carboxylate groups appearing between 503 and 686 cm^{-1}. A weak CH_2 stretching vibration was detected at 2962.4 cm^{-1} in FTIR, and a more prominent CH_2 stretch at 2996.4 cm^{-1} was noted in the Raman spectrum. The amino acid combination band were observed at 2170.3 cm^{-1}, while strong NH_3^+ vibrations lies in the range of 1497.2–1577.5 cm^{-1}, while NH_3^+ stretching modes were present in the 2791.4–2887.5 cm^{-1} range.

Nitrate groups were also identified, with the symmetric stretching band of NO_3^- observed at 1043.2 cm^{-1} and the asymmetric stretch at 1386.1 cm^{-1}. Figure 6 presents the Raman spectrum of GPCN, which helps confirm and complement the FTIR findings. Modes such as rocking, wagging, and bending of CH_2 and NH_3^+ groups; symmetric stretching of the CCN backbone; and scissoring and twisting motions were all evident. Together, FTIR and Raman analyses confirmed functional groups and structural composition of the newly grown GPCN crystal. The comparative assignments of FTIR and Raman, illustrates in Table 3.

Table 3 Comparative FTIR and Raman Assignments

IR (υ cm^{-1})	Raman (υ cm^{-1})	Assignments
-	103.6	Lattice vibrations
-	150.3	Lattice vibrations
503.1	502.3	COO^- rocking
557.5	551.2	M-N bond
607.8	606.9	COO^- bending
686.0	682.3	COO^- wagging
889.6	892.2	CNN symmetric stretching
929.7	929.4	CH_2 wagging
1043.2	1049.1	NO_3^- symmetric stretch
1127.1	1128.0	NH_3^+ rocking

ISBN: 978-93-95369-55-8 (paperback) 978-93-95369-46-6 (electronic) | © 2025 Advent Publishing.

1158.7	1153.9	NH_3^+ rocking
1322.9	1320.7	CH_2 wagging/ twisting
-	1336.2	NO_3^- asymmetric stretch
1386.1	1391.0	NO_3^- asymmetric stretch
1437.1	1438.2	CH_2 scissor
1497.2	1498.1	NH_3^+ deformation
1577.5	1579.7	NH_3^+ deformation
2170.3	2172.4	Amino acid combination band
2229.2	2222.3	Amino acid combination band
2273.9	2289.4	Amino acid combination band
2605.5	2605.0	N-H bonded oscillation
2791.4	2795.5	NH_3^+ stretch
2887.5	2865.3	NH_3^+ stretch
2962.4	2967.8	CH_2 stretching
-	2996.4	CH_2 stretching
3105.8	3108.9	NH_3^+ stretching

3.5. UV–Vis Spectral Analysis

The UV–Vis absorption spectrum of the GPCN crystal was recorded using a Hitachi U-2900 spectrophotometer across the wavelength range of 100–1200 nm, encompassing both the ultraviolet and visible regions[11,15]. As shown in Figure 7, a distinct absorption peak is observed between 200–212 nm, attributed to the n–π∗ electronic transition[19]. The cutoff wavelength (λ_{max}) was measured at 216 nm, corresponding to an estimated optical band gap of 5.75 eV. The crystal shows broad transparency range from 250 to 1200 nm, with minimal absorption across this region, making it well-suited for diverse optoelectronic and photonic applications.

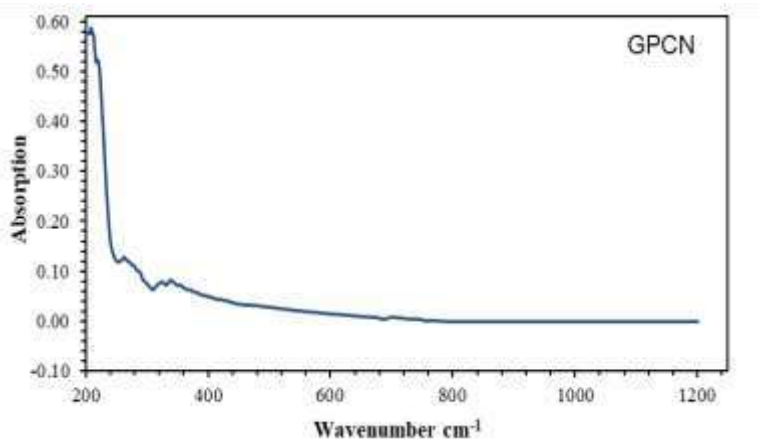

Fig. 7. UV plot of GPCN crystal.

ISBN: 978-93-95369-55-8 (paperback) 978-93-95369-46-6 (electronic)

3.6. Second Harmonic Generation Studies

The nonlinear optical (NLO) response of the grown GPCN crystals was assessed using the standard Kurtz and Perry powder technique to evaluate second harmonic generation (SHG) efficiency[16]. The crystals were ground to an average particle size of 125–150 μm and compacted between two transparent glass slides. The powdered sample was then irradiated with a pulsed Q-switched Nd:YAG laser operating at a fundamental wavelength of 1064 nm. Upon excitation, a green emission at 532 nm was observed, confirming frequency doubling—a definitive characteristic of SHG-active materials. The output signal was monitored using a cathode ray oscilloscope. The GPCN sample produced an SHG output of 123 mV, whereas the standard potassium dihydrogen phosphate (KDP) crystal under identical experimental conditions gave an output of 185 mV, using an input energy of 2.69 mJ per pulse. This shows that the SHG efficiency of GPCN is approximately 0.66 times that of KDP. It is important to note that SHG efficiency can vary depending on several factors, including the purity of the material, particle size, crystallinity, growth quality, and experimental setup. The results confirm that GPCN exhibits moderate nonlinear optical properties, making it a promising candidate for photonic and laser-based applications[13].

3.7. I–V and Photoconductivity Characteristics

The current–voltage (I–V) and photoconductivity characteristics of the grown GPCN crystal were examined to evaluate its electrical behavior under both dark and illuminated conditions. Measurements were performed using a high precision digital pico-ammeter. Polished crystal samples with a thickness of 4 mm were prepared, with opposite faces silver-coated to ensure good electrical contact. The samples were placed between two copper electrodes in a parallel plate configuration for the measurements of corresponding current, with applying a DC voltage ranging from 0 to 30 V.

Photoconductivity measurements were carried out by illuminating the crystal with a 100 W tungsten filament lamp filled with iodine vapor. The dark current was measured by shielding the sample with a black cloth, while the bright current was measured under illumination. The I–V plots (Figure 8) show a linear rise in current with applied voltage up to an electric field of 50 V/cm, beyond which the current increased sharply, indicating non-ohmic behavior. Based on these results, the safe operating voltage for the crystal is estimated to be around 30 V.

Interestingly, the GPCN crystal exhibited **negative photoconductivity,** as the current under dark conditions was found to be higher than that under illumination. This phenomenon suggests a reduction in charge carrier mobility or density when exposed to light. According to the Stockmann model, this behavior can be attributed to recombination centers or trapping states within the crystal that become more active under illumination, leading to a decrease in free charge carriers. In the present study, dark current was found to be large than the bright current, indicating the occurrence of negative photoconductivity[20].

ISBN: 978-93-95369-55-8 (paperback) 978-93-95369-46-6 (electronic) | © 2025 Advent Publishing.

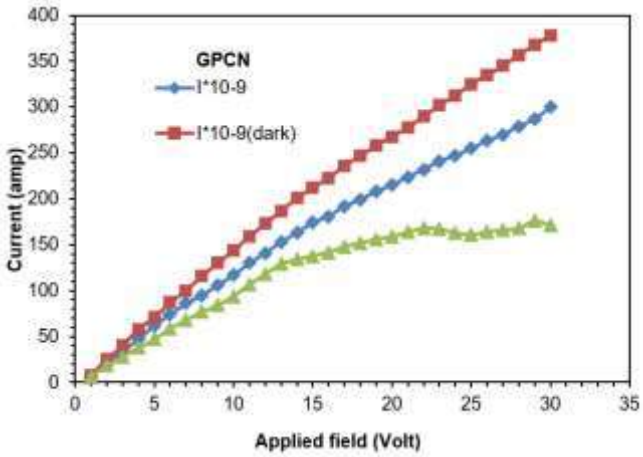

Fig. 8. I–V and Photoconductivity characteristic of GPCN crystal

3.8. SEM Analysis

The surface morphology of the grown GPCN crystal were analyzed using a Scanning Electron Microscope (JSM-840) [21]. The SEM image reveal a smooth, uniform surface devoid of visible cracks, voids, valleys, or major dislocation networks, indicating high crystalline quality. In certain localized regions, small micro crystallites were observed, which may be attributed to the incorporation of calcium ligands during the crystal growth process (Figure 9). Additionally, scattered white spots on the surface are likely due to the incorporation of chlorine atoms into the crystal matrix. No surface damage or major defects were detected upon further magnification, confirming the mechanical stability and surface perfection of the GPCN crystal. These results validate the successful growth of high-quality crystals suitable for further optical and electronic applications.

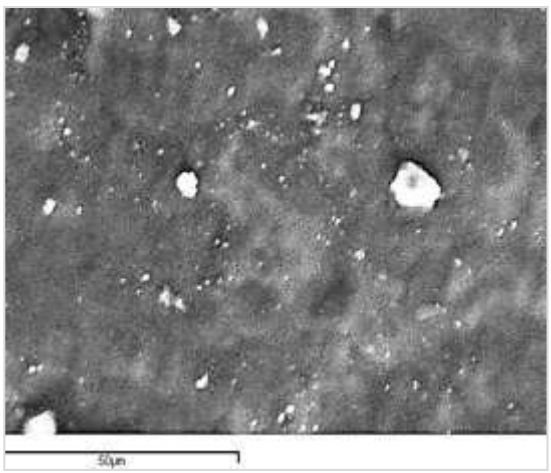

Fig. 9. SEM of grown GPCN crystal.

ISBN: 978-93-95369-55-8 (paperback) 978-93-95369-46-6 (electronic)

3.9. Dielectric studies

An HP-LCZ meter (Model 4277A) was used to test the dielectric of the generated GPCN crystals between 100 Hz and 1 MHz. Using the formulas[19], ε' = Ct / ε₀A, and ε" = D×ε', where Ct is the measured capacitance, A is the crystal's area, ε₀ is the vacuum permittivity, and D is the dissipation factor, the dielectric constant (ε') and dielectric loss (ε") were determined.

The results, illustrated in Figure 10, show that the dielectric constant is relatively high at lower frequencies but decreases sharply as frequency increases. This behavior is primarily attributed to space charge, orientational, electronic, and ionic polarizations, which are more active at low frequencies [22]. As the frequency increases, these polarization mechanisms cannot keep pace with the applied field, resulting in a decrease in ε'. The dielectric loss (ε"), shown in Figure 11, also decreases with frequency, indicating minimal energy dissipation at higher frequencies. This low dielectric loss signifies good crystal quality, making the GPCN crystal suitable for non-linear optical and high-frequency device applications.

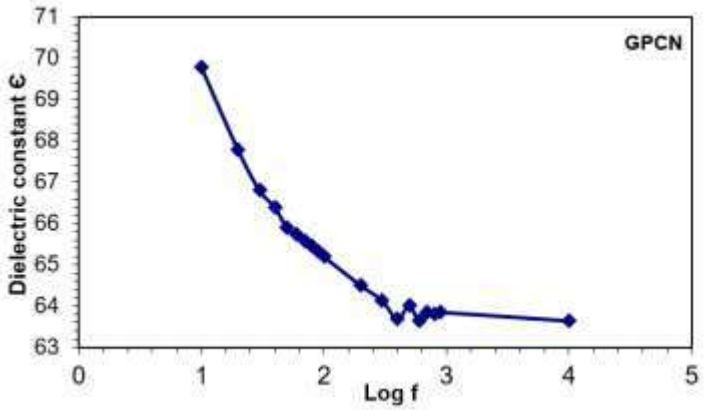

Fig. 10. Dielectric constant Vs log frequency of GPCN crystal.

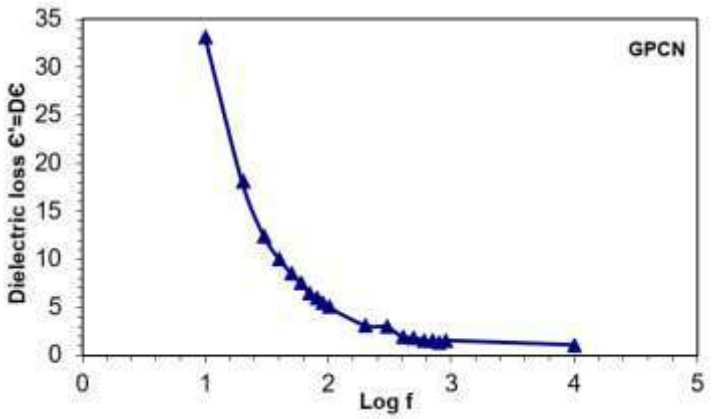

Fig. 11. Dielectric loss Vs log frequency of GPCN crystal.

ISBN: 978-93-95369-55-8 (paperback) 978-93-95369-46-6 (electronic)

3.10. Micro-hardness Measurement

A LECO-Vickers microhardness tester fitted with a diamond indenter was used to assess the microhardness of the GPCN crystals that had developed. Loads ranging from 10 g to 300 g were applied to a well-polished crystal on the testing platform, with a dwell duration of 10 seconds[17]. When determining whether optical crystals are suitable for device manufacture, microhardness—a crucial mechanical property that shows a material's resistance to localized deformation—is essential. The average diagonal lengths of the imprints were measured for additional study after indentations were created at different stresses. The Vickers Hardness Number (VHN) was calculated using the standard formula,

$$H_v = \frac{1.854\,P}{d^2}\frac{Kg}{mm^2}$$

where P is the applied load (in kg) and d is the average diagonal length (in mm). The VHN was observed to increase nonlinearly with load and reached a maximum value of 72.2 kg/mm² at 50 g. However, beyond this load, especially at 100 g, micro-cracks started to appear (Figure 12).

To assess the work hardening behavior, the work hardening coefficient '*n*' was determined from the slope of a log P vs. log d plot (Figure 13). The obtained value of n = 6.27 indicates that materials belongs to the soft category.

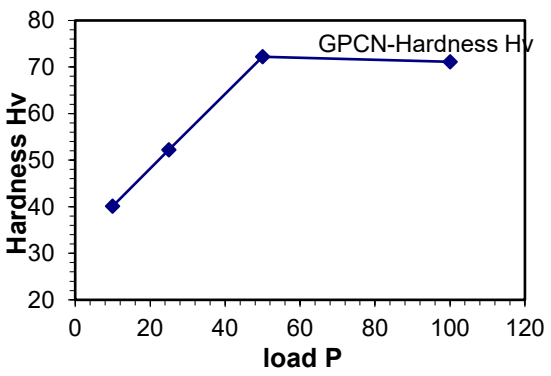

Fig. 12. VHN Vs load plot.

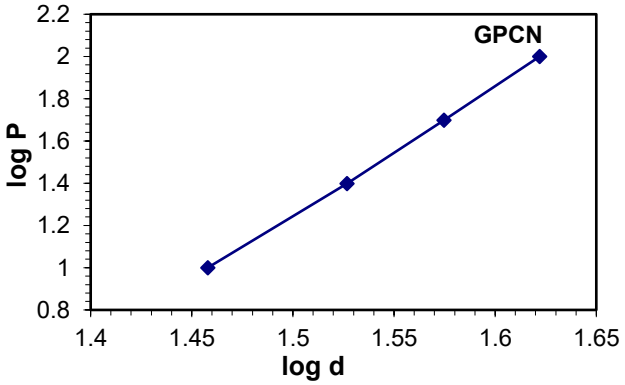

Fig. 13. Log P Vs Log d plot.

4. Conclusion

The slow evaporation method was successfully used to create transparent crystals of acid-mixed glycine–potassium–calcium nitrate (GPCN) at room temperature. Favorable circumstances for crystal formation were indicated by the compound's linear increase in solubility over the 300–350 K temperature range. The sample's chemical composition was verified by CHN and EDAX analyses. The crystal's orthorhombic symmetry was determined by powder X-ray diffraction (XRD) examination. Its unit cell volume was 1961.30 Å³, and its lattice parameters were a = 14.827 Å, b = 13.287 Å, and c = 9.954 Å.

ISBN: 978-93-95369-55-8 (paperback) 978-93-95369-46-6 (electronic)

Nuclear Magnetic Resonance (NMR) studies, confirmed the presence of NH_2 and CH_2 groups in the molecular framework, suggesting the incorporation of glycine in zwitterion form. FTIR and Raman spectral analyses identified key functional groups, with overlapping peaks indicating the absence of a center of symmetry in the molecule.

UV–Vis spectroscopy revealed that the crystal possesses a broad transparency range from 350 nm to 1200 nm, with a cut-off wavelength at 216 nm and an optical band gap of 5.75 eV, indicating its potential suitability for optoelectronic applications. Second Harmonic Generation (SHG) testing using the Kurtz and Perry method confirmed nonlinear optical behavior, with SHG efficiency measured at 0.66 times that of standard KDP crystals.

Electrical characterization through I–V and photoconductivity measurements revealed a linear increase in current with applied voltage up to 30 V. Interestingly, the material exhibited negative photoconductivity upon light exposure, attributed to recombination of charge carriers.

Scanning Electron Microscopy (SEM) showed smooth crystal surfaces with minimal defects, confirming high-quality crystal growth. Dielectric studies exhibited a high dielectric constant at low frequencies and decreasing loss at high frequencies, indicating good optical quality. Micro hardness measurements yielded a work hardening coefficient of 6.27, categorizing the crystal as a soft material.

Overall, the GPCN crystal demonstrates promising structural, optical, electrical, and mechanical properties suitable for optoelectronic and nonlinear optical device applications.

5. References

1. J. H. Paredes, D. G. Mintik, O. H. Negrete, H. E. Ponce, M. E. Alvarez, R. R. R. Mijangos, and A. D. Moller, *J. Phys. Chem. Solids*, 2008, 69,1974.
2. J. H. Paredes, D. G. Mintik, O. H. Negrete, H. E. Ponce, M. E. A. Ramos, and A. D. Moller, *J. Mol. Struct.*, 2008, 875, 295.
3. R. Pepinsky, Y. Okaya, D. P. Eastman, and T. Mitsui, *Phys. Rev.*, 1957,107, 1538.
4. M. M. Khandpekar and S. P. Pati, *J. Opt. Commun.*, 2010, 283, 2700.
5. D. Eimert, S. Velsko, L. Davis, F. Wang, G. Loiaceono, and G. Kennedy, *IEEE J. Quantum Electron.*, 1989, 25,179.
6. M. D. Agarwal et al., *J. Cryst. Growth*, 1999, 204, 179.
7. M. N. Bhat and S. M. Dharmaprakash, *J. Cryst. Growth*, 2002, 235, 511.
8. J. K. Mohan Rao and M. A. Vishwamitra, *Acta Crystallogr. B*, 1972, 28, 1484.
9. S. Natarajan, *Z. Kristallogr.*, 1983, 163, 305.

ISBN: 978-93-95369-55-8 (paperback) 978-93-95369-46-6 (electronic)

10. R. V. Krishnakumar, M. S. Naandhini, S. Natarajan, K. Sivakumar, and B. Varghese, *Acta Crystallogr. C*, 2001, 57, 1149.
11. S. A. Martin Britto and S. Natarajan, *Opt. Commun.*, 2008, 281, 457.
12. S. Dhanuskodi and K. Vasanta, *Spectrochim. Acta A*, 2005, 61, 1777.
13. T. Mallik and T. Kar, *J. Cryst. Growth*, 2005, 274, 251.
14. S. Dhanuskodi, A. P. Jeyakumari, and S. Manivannan, *J. Cryst. Growth*, 2005, 282, 72.
15. S. Manikandan and S. Dhanuskodi, *Spectrochim. Acta A*, 2007, 67, 160.
16. S. K. Kurtz and T. T. Perry, " *J. Appl. Phys.*, 1968, 39, 3798.
17. A. J. A. Pragasam, J. Mhadavan, M. G. Mohamed, S. Selvakumar, K. Ambujan, and P. Sagayaraj, *Opt. Mater.*, 2009, 29, 173.
18. R. M. Silverstein, G. C. Bassler, and C. Morrk, *Spectrometric Identification of Organic Compounds*, 4th ed., Wiley, USA, 1991.
19. T. Balakrisnan and K. Ramamurthi, *Cryst. Res. Technol.*, 2006, 12, 1184.
20. R. H. Bube, *Photoconductivity of Solids*, Wiley, New York, 1981.
21. S. Suresh, A. Ramanand, P. Mani, and K. Murhyanand, *J. Optoelectron. Biomed. Mater.*, 2010, 1, 129.
22. C. Balarew and R. Duhew, *J. Solid State Chem.*, 1984, 55, 1

ISBN: 978-93-95369-55-8 (paperback) 978-93-95369-46-6 (electronic)